Supporting Information

Response of organic aerosol characteristics to emission reduction in Yangtze River Delta region

Jinbo Wang[1,2], Jiaping Wang[1,2,3*], Wei Nie[1,2,3], Xuguang Chi[1,2,3], Dafeng Ge[1,2], Caijun Zhu[1,2], Lei Wang[1,2,3], Yuanyuan Li[1,2], Xin Huang[1,2], Ximeng Qi[1,2,3], Yuxuan Zhang[1,2,3], Tengyu Liu[1,2,3] and Aijun Ding[1,2,3]

[1]Joint International Research Laboratory of Atmospheric and Earth System Sciences, School of Atmospheric Sciences, Nanjing University, Nanjing, 210023, China.

[2]Jiangsu Provincial Collaborative Innovation Center of Climate Change, Nanjing, 210023, China.

[3]National Observation and Research Station for Atmospheric Processes and Environmental Change in Yangtze River Delta, Nanjing, Jiangsu Province, China

Corresponding author: Jiaping Wang (wangjp@nju.edu.cn)

Figures

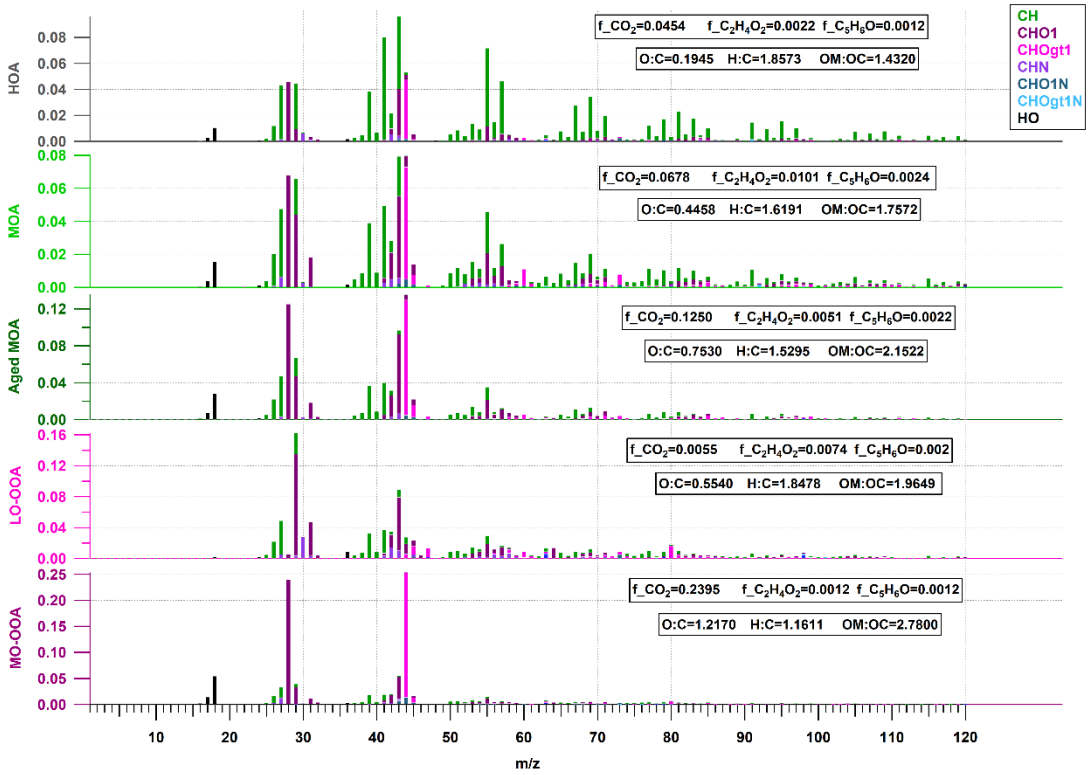

Figure S1. High resolution mass spectra of the PMF-resolved OA factors. The fraction of tracer ions (CO_2^+, $C_2H_4O_2^+$ and $C_5H_6O^+$) is shown in the text box for each factor, together with the elemental composition including oxygen-to-carbon ratio (O:C), hydrogen-to-carbon ratio (H:C) and organic-matter to organic-carbon ratio (OM:OC).

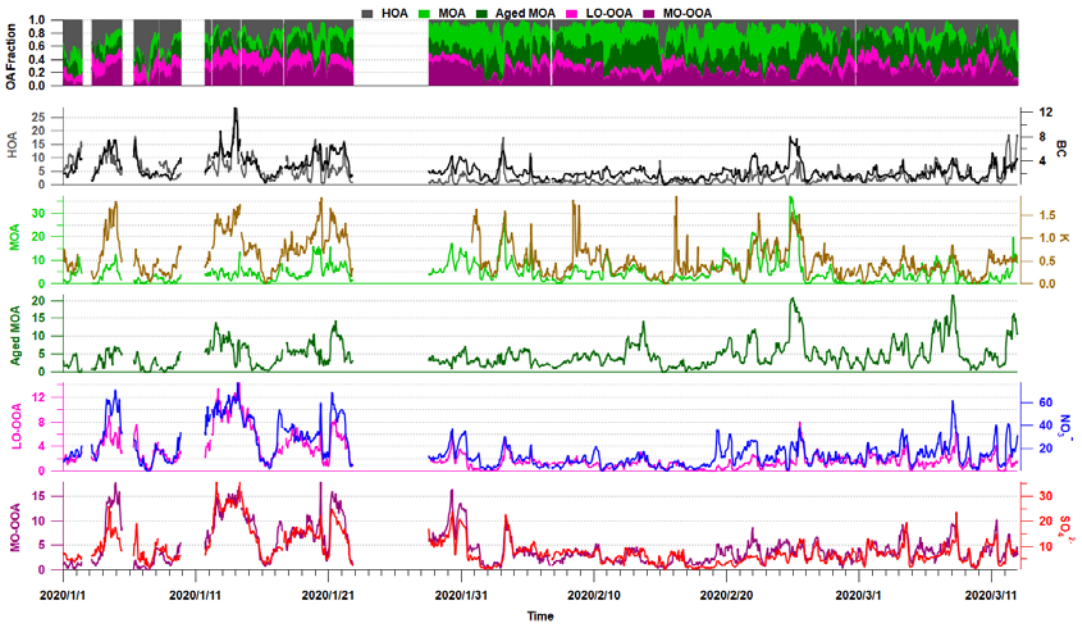

Figure S2. Time series of PMF factors, related species and the fraction of PMF factors. The related species are black carbon (BC), potassium (K), nitrate (NO_3^-), sulfate (SO_4^{2-}), respectively. The unit of OA factors and related species concentration is μg/m^3.

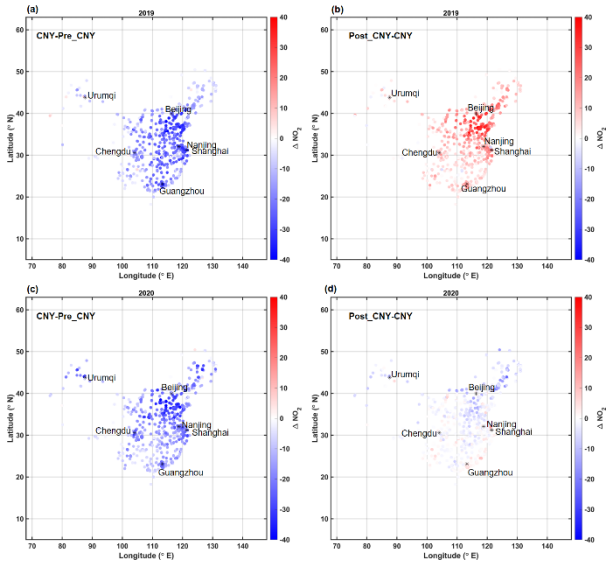

Figure S3. Change of NO_2 concentration before and after CNY holiday. The unit is μg/m^3. (a) and (c) change of NO_2 concentration during CNY holiday minus that before CNY holiday in 2019 and 2020, respectively; (b) and (d) change of NO_2 concentration after CNY holiday minus that during CNY holiday in 2019 and 2020, respectively. The underlying graph is reference grid for longitude and latitude, and not involved with coastline, boundary line or any other boundaries.

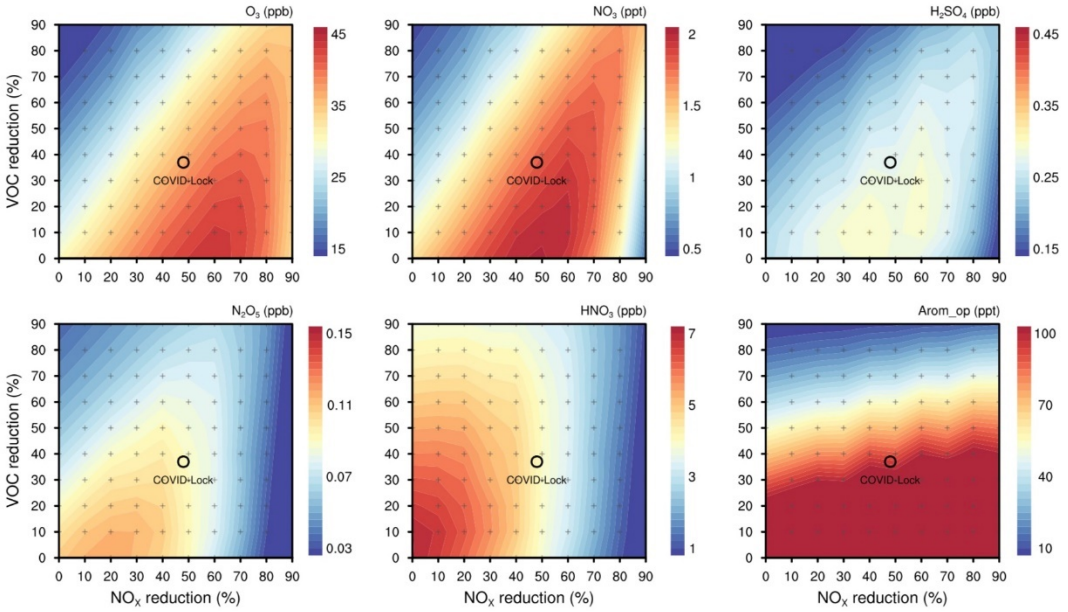

Figure S4. Empirical kinetic modeling approach (EKMA) isopleths of changes of O_3, NO_3 radical, H_2SO_4, N_2O_5, HNO_3 and oxidization products of aromatics (Arom_op) as a function of VOCs and NO_x emission reduction in eastern China during the COVID lockdown period. The circles represent the averaged emission reduction rate of VOCs and NO_x during lockdown.

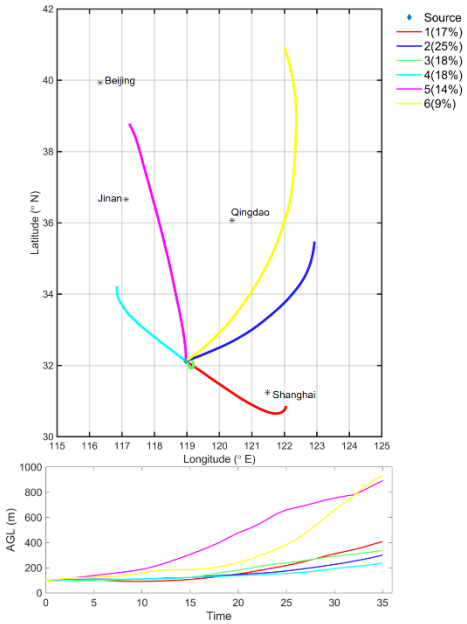

Figure S5. The backward trajectory for different airmass clusters. The No.1 trajectory (red line) represents YRD airmass, the No.3 trajectory (green line) represents local airmass. The airmass clusters represented by the No.4 trajectory (aqua line) and No.5 trajectory (purple line) were treated as whole (northern airmass). The underlying graph is reference grid for longitude and latitude, and not involved with coastline, boundary line or any other boundaries.

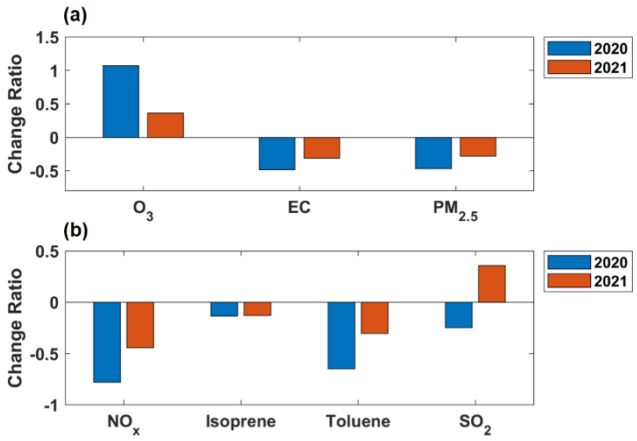

Figure S6. Change rate of (a) O_3, element carbon (EC) and $PM_{2.5}$ concentration (b) NO_x, isoprene, toluene and SO_2 mixing ratio during reduced emission stages (RES) in 2020 and 2021. The normal emission stages (NES) are from 1st January to 23th January in 2020 (i.e., Pre-COVID) and from 28th January to 10th February in 2021. The RES are from 28th January to 17th February in 2020 (i.e., COVID-lock) and from 15th February to 28th February in 2021, not including the first few days of CNY. The post-emission-reduction stage is from 18th February to 12th March in 2020 (i.e., Post-COVID). The formula to calculate change rate of species X is $(X_{RES} - X_{NES})/ X_{NES}$.

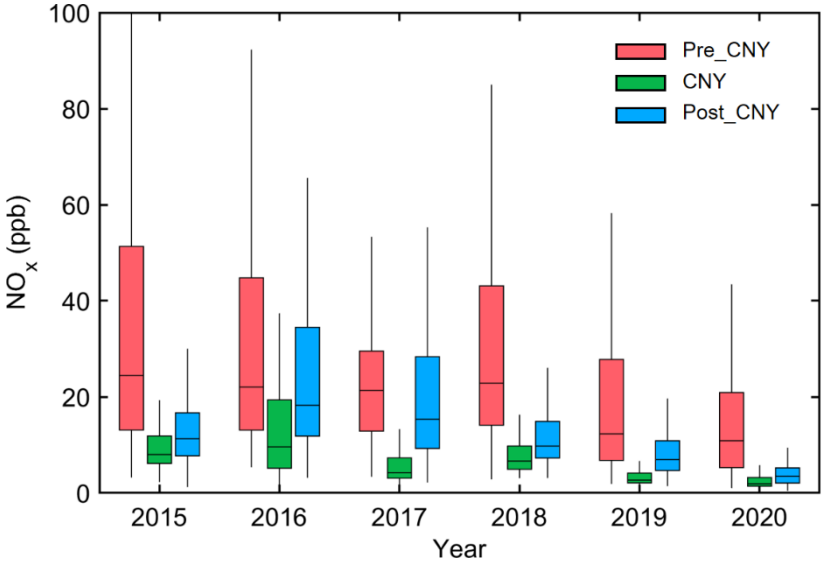

Figure S7. Comparison of NO_x concentration during different periods (before CNY, during CNY and post CNY) from 2015 to 2020. Box plots represent the 25th and 75th percentile and the whiskers stand for maximum and minimum values.

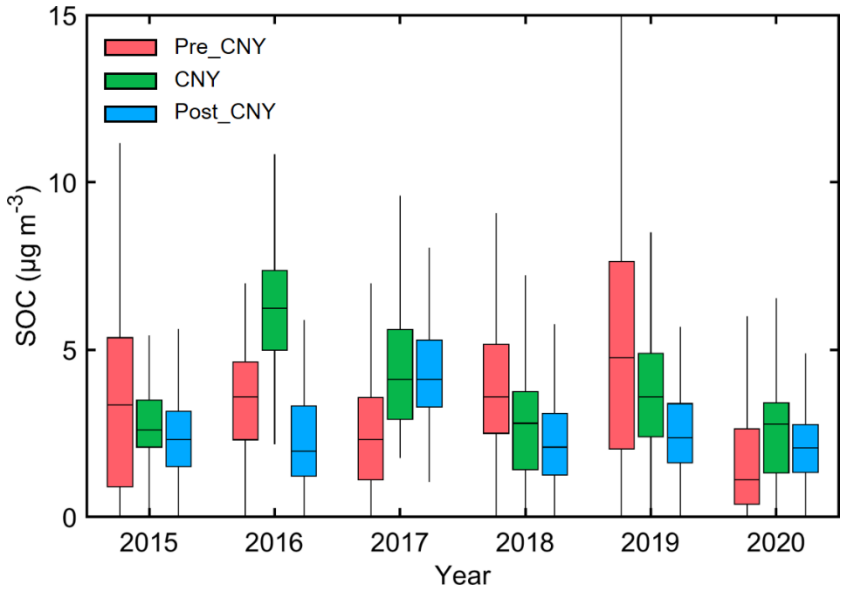

Figure S8. Comparison of secondary organic carbon (SOC) during different periods (before CNY, during CNY and post CNY) from 2015 to 2020. Box plots represent the 25th and 75th percentile and the whiskers stand for maximum and minimum values.

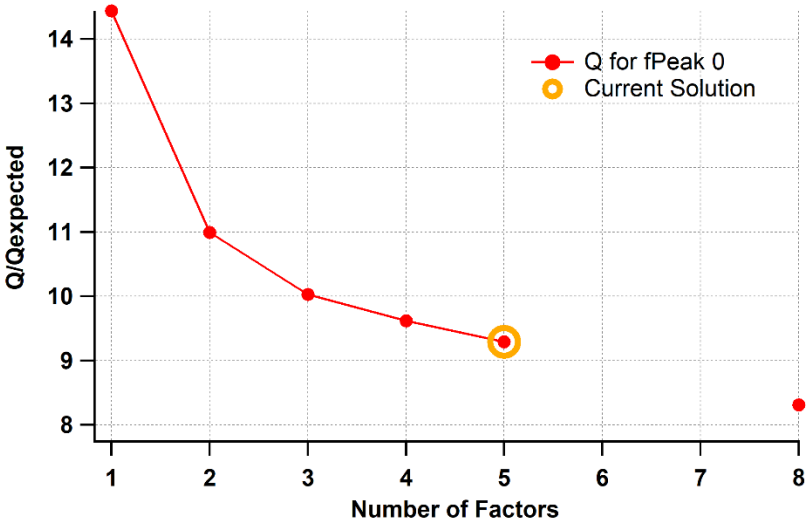

Figure S9. Q/Q_{exp} as a function of number of factors selected for PMF modeling.

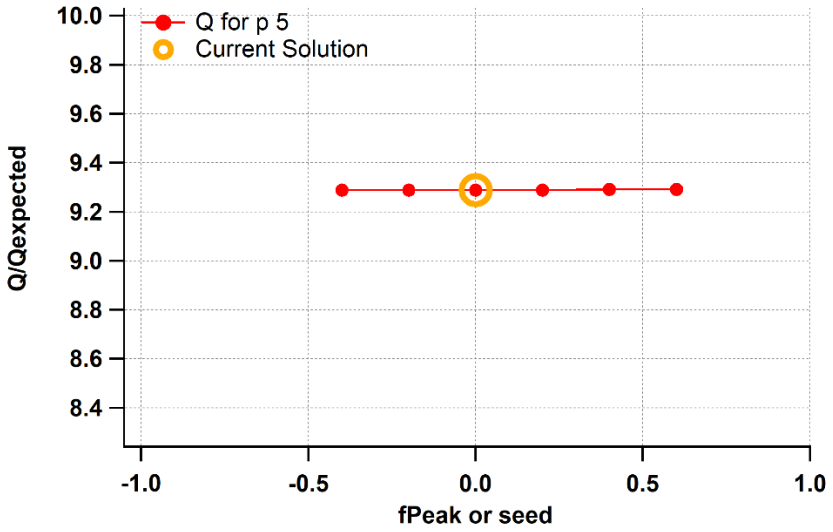

Figure S10. For the 5-factor solution, Q/Q_{exp} as a function of fPeak.

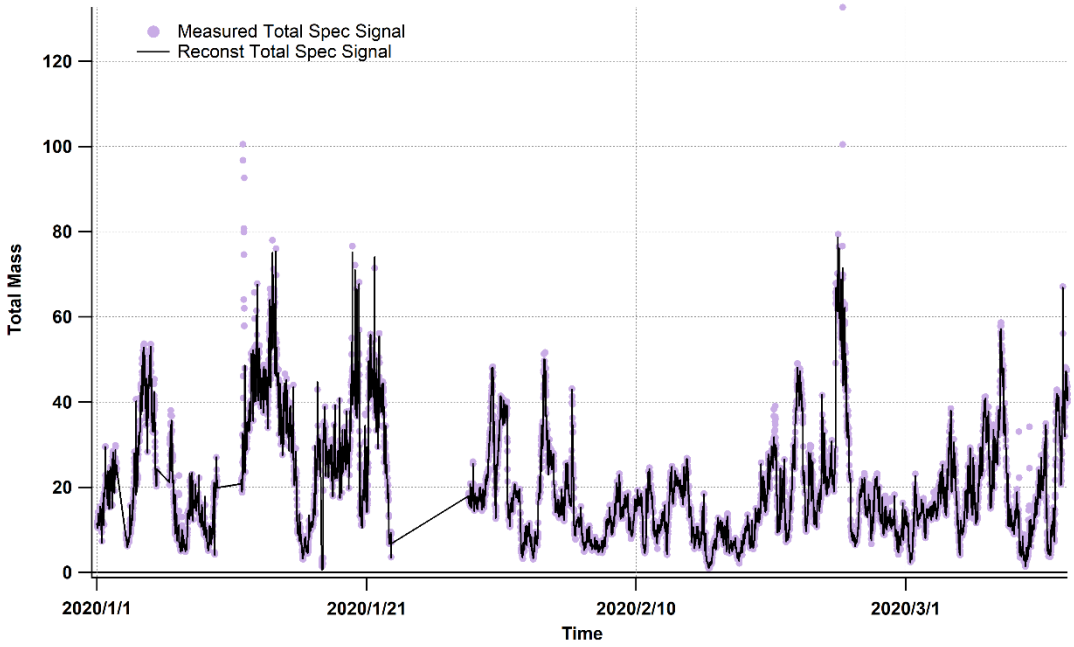

Figure S11. For the 5-factor solution, time series of the measured organic mass and the reconstructed organic mass (the sum of the 5 factors). The unit is $\mu g/m^3$.

Sections

Section S1

Fig. S1 shows the mass spectrum, fraction of tracer ions signal and elemental composition of OA factors. The CO_2^+, $C_2H_4O_2^+$ and $C_5H_6O^+$ are tracer ions of OOA, biomass burning (BB) and IEPOX-SOA (isoprene epoxydiols-derived secondary organic aerosol). The first factor is HOA (hydrocarbon-like OA) originated directly from combustion process because it has significantly high signal of $C_4H_7^+$ and $C_4H_9^+$ (Fig. S1). Besides, time series of this factor correlates well with BC which is a primary pollutant (Fig. S2). The Pearson Correlation Coefficients (r_{BC}) is 0.69. The other factors are OOA which have higher signal of CO_2^+ or CHO^+. The second and third factor are special OOA, which are likely to be affected by transported airmass significantly. The source of the two factors is more various than other factors because OA from multiple sources tends to mix well during transport. It is noted that the two factors correlate well to $C_2H_4O_2^+$ and $C_5H_6O^+$ concurrently (Fig. S3), although the two ions represent entirely different OA source as mentioned above. The second factor is named as MOA (mixing OA). The spectrum of MOA has higher signal of CO_2^+ but includes some hydrocarbon ions, influenced by mixed-well airmass and mixed emission source. The fraction of BB tracer ions $C_2H_4O_2^+$ signal is slightly lower than typical BBOA in its mass spectrum (Aiken et al., 2009), but it correlates well with BB tracer potassium (r_k=0.5), showing the apparent contribution from BB. The third factor has higher oxygen-to-carbon ratio and lower hydrogen-to-carbon ratio than MOA (Fig. S1). Considering that the profile of this factor relates to MOA (r=0.93) and time series of this factor relates to $C_2H_4O_2^+$ and $C_5H_6O^+$ closely, it was thought to be Aged MOA. The fourth and fifth factors are more aged SOA (less oxidized oxygenated OA, LO-OOA and more oxidized oxygenated OA, MO-OOA). The correlation coefficient of the two factors (r=0.75) is highest of all factors. The two factors both highly correlate to secondary inorganic aerosol (LO-OOA: $r_{nitrate}$=0.85, $r_{sulfate}$=0.92; MO-OOA: $r_{nitrate}$=0.90, $r_{sulfate}$=0.87). There is higher fraction of CHO^+ ions in the spectrum of LO-OOA (Fig S1). Furthermore, the MO-OOA is the most oxygenated OA of all factors.

Section S2

As Fig. S6 shows, air pollutant also changed substantially during the same period in 2021 mainly

caused by Chinese New Year (CNY). The primary pollutant (EC, NO_x, toluene and SO_2) and $PM_{2.5}$ concentration decreased because the traffic was not so busy as usual, some factories shut and people stayed at home during CNY holiday. The natural volatile organic compounds did not change obviously but the O_3 increased when human activities were minimized in 2020 and 2021. The amount of O_3 increase is different in the two years because the decline in emission was less without lockdown in 2021. The result confirms again that the decreased NO_x will boost O_3 concentration. It also notes that the more NO_x reduction causes more O_3 enhancement. The NO_x-induce O_3 enhancement is affected by the intensity of emission change.

Section S3

Fig. S7 presents the comparison of NO_x before, during and after CNY holiday in six years (from 2015 to 2020) at SORPES station. The change rule of NO_x is similar in these years. The NO_x was most before CNY, reducing during CNY and recovering after CNY. The result demonstrates that primary emission also decreased to a large extent during common holiday, besides periods covered by voluntary emission control.

Section S4

Based on multi-year OC/EC measurements at SORPES site from 2015 to 2020, we estimated the secondary organic carbon (SOC) using the EC-tracer method(Turpin and Huntzicker, 1995; Cheng et al., 2014; Feng et al., 2022) with the following equations.

$$POC = (OC/EC)_{pri} \times EC \quad (1)$$

$$SOC = OC_{total} - POC \quad (2)$$

where POC is primary organic carbon and $(OC/EC)_{pri}$ is the ratio of primary OC/EC. We adopted the lowest 10% of OC/EC value as $(OC/EC)_{pri}$ in this study. OC_{total} represents the measured OC concentration. Fig. S8 presents the comparison of SOC before, during and after CNY holiday in six years.

Section S5

The key diagnostic plots of the AMS-PMF outcomes are shown in Fig. S9-S11. We selected the 5-factor solution with fPeak = 0 as the best solution because O/Q_{exp} didn't decrease significantly when the number of factors ≥5. The 4-factor solution would combine MOA and aged MOA into one factor, the 6-factor and 7-factor solution would diverge, and the 8-factor solution would split the MOA, aged MOA and MO-OOA into more factors which couldn't be reasonably explained when the correlation between the factors and external tracers (fragments, inorganic components, etc.) was analyzed. Moreover, the reconstructed total mass concentration of OA can well match the measured total mass concentration of OA, revealing that the result of the 5-factor solution is appropriate.

The mixed OA factors are not only found in the 5-factor solution but also appeared in PMF results with more large number of factors, which implicates that these factors are true and stable components of local OA.

References

Aiken A C, Salcedo D, Cubison M J, Huffman J A, Decarlo P F, Ulbrich I M, Docherty K S, Sueper D, Kimmel J R, Worsnop D R, Trimborn A, Northway M, Stone E A, Schauer J J, Volkamer R M, Fortner E, De Foy B, Wang J, Laskin A, Shutthanandan V, Zheng J, Zhang R, Gaffney J, Marley N A, Paredes-Miranda G, Arnott W P, Molina L T, Sosa G, Jimenez J L (2009). Mexico City aerosol analysis during MILAGRO using high resolution aerosol mass spectrometry at the urban supersite (T0) - Part 1: Fine particle composition and organic source apportionment. Atmospheric Chemistry and Physics, 9(17): 6633-6653

Cheng Y, He K B, Duan F K, Du Z Y, Zheng M, Ma Y L (2014). Ambient organic carbon to elemental carbon ratios: Influence of the thermal-optical temperature protocol and implications. Science of the Total Environment, 468: 1103-1111

Feng Z M, Zheng F X, Liu Y C, Fan X L, Yan C, Zhang Y S, Daellenbach K R, Bianchi F, Petaja T, Kulmala M, Bao X L (2022). Evolution of organic carbon during COVID-19 lockdown period: Possible contribution of nocturnal chemistry. Science of the Total Environment, 808

Turpin B J, Huntzicker J J (1995). Identification of secondary organic aerosol episodes and quantitation of primary and secondary organic aerosol concentrations during SCAQS. Atmospheric Environment, 29(23): 3527-3544